
HM-DF SNN: Transcending Conventional Online Learning with Advanced Training and Deployment

Zecheng Hao¹, Yifan Huang¹, Zijie Xu^{1,2}, Wenxuan Liu¹, Yuanhong Tang¹,
Zhaofei Yu^{1,2*} & Tiejun Huang^{1,2}

¹ School of Computer Science, Peking University

² Institute for Artificial Intelligence, Peking University

Abstract

Spiking Neural Networks (SNNs) are considered to have enormous potential in the future development of Artificial Intelligence due to their brain-inspired and energy-efficient properties. Compared to vanilla Spatial-Temporal Back-propagation (STBP) training methods, online training can effectively overcome the risk of GPU memory explosion. However, current online learning framework cannot tackle the inseparability problem of temporal dependent gradients and merely aim to optimize the training memory, resulting in no performance advantages compared to the STBP training models in the inference phase. To address the aforementioned challenges, we propose Hybrid Mechanism-Driven Firing (HM-DF) model, which is a family of advanced models that respectively adopt different spiking calculation schemes in the upper-region and lower-region of the firing threshold. We point out that HM-DF model can effectively separate temporal gradients and tackle the mismatch problem of surrogate gradients, as well as achieving full-stage optimization towards computation speed and memory footprint. Experimental results have demonstrated that HM-DF model can be flexibly combined with various techniques to achieve state-of-the-art performance in the field of online learning, without triggering further power consumption.

1 Introduction

Spiking Neural Networks (SNNs), as the third-generation neural network towards brain-inspired intelligence [32], have gained widespread attention from researchers in Artificial Intelligence community. SNNs utilize spiking neurons as the basic computing unit to transmit discrete spike firing sequences to the post-synaptic layer. Due to the fact that spiking neurons only emit spikes when the membrane potential exceeds the firing threshold, compared to the activation values in traditional Artificial Neural Networks (ANNs), spike sequences have sparse and event-driven properties, which can demonstrate superior computational efficiency and power consumption ratio on neuromorphic hardware [34, 4, 36].

Spatial-Temporal Back-propagation (STBP) is the most significant training algorithm in the supervised learning domain of SNNs currently [44]. By introducing the concepts of temporal dimension and surrogate gradient, STBP simultaneously tackles the Markov property and non-differentiable problem of SNNs existed in the forward propagation and firing process. However, although STBP training has significantly improved the learning performance and universal property of SNNs [43, 37, 39], as its back-propagation chains are inseparable due to the temporal dependencies, its GPU memory will inevitably boost linearly with the number of time-steps. This phenomenon greatly increases the training burden and hinders the further application of SNNs to complex scenarios [25, 48] and advanced spiking models [16, 21].

*Corresponding author: yuzf12@pku.edu.cn

To address this problem, researchers have transferred the idea of online learning to the STBP training framework [46, 33], which means that by detaching the temporal dependent gradient terms, SNNs can immediately perform back-propagation at any time-step. This scheme ensures that the corresponding GPU memory is independent of the training time-steps and remains constant, effectively alleviating the problem of computation memory explosion. However, the current proposed methods based on online learning still have **three main defects**: (i) the discrepancy between forward and backward propagation, (ii) ineffective online deployment, (iii) the mismatch problem of surrogate gradients.

The reason for the first defect is that the surrogate function of spiking neurons is generally related to the value of membrane potential and the spike sequence is usually unevenly distributed in the temporal dimension, making the temporal dependent gradients different from each other and unable to merge with the back-propagation chain along the spatial dimension. In this case, when online learning frameworks detach temporal dependent gradients, it will lead to inconsistency between forward and backward propagation, resulting in learning performance degradation. The second defect refers to the fact that current online learning methods mainly focus on optimizing training memory, but cannot bring any optimization regarding computation time or memory during the inference phase. This is because under the framework of firing binary spikes, it is difficult to introduce parallel computation or weight compression techniques to improve inference speed or optimize memory usage without sacrificing learning precision. While the third problem, as an inherent defect of vanilla STBP training, when combined with the two points mentioned above, will further suppress the performance of conventional online learning methods.

Based on the above discussion, we propose Hybrid Mechanism-Driven Firing (HM-DF) model for online training. On the one hand, HM-DF model completely solves the non-differentiable problem of the firing process and enhances the uniformity of the spike sequence, significantly improving the separability and alignment degree of backward gradients compared to vanilla spiking models. On the other hand, it can be flexibly combined with various techniques for optimizing computational costs, achieving full-stage optimization including training and inference phases **without increasing power consumption**. Our contributions are summarized as follow:

- Compared to vanilla spiking models, we theoretically point out that HM-DF model has more superior gradient separability and alignment, which is conducive to achieving high-performance online learning.
- We further propose variant versions for HM-DF model. Among them, the HM-DF model based on membrane potential batch-normalization can more effectively regulate the degree of gradient separability and be reparameterized into vanilla HM-DF model in the inference phase. In addition, it can further improve the network performance by combining channel attention mechanism.
- By combining random back-propagation, parallel computation and other techniques, HM-DF model can achieve comprehensive optimization in terms of time and memory overhead during training and inference phases, which goes beyond the optimization scope of vanilla online training.
- We achieve state-of-the-art (SoTA) performance on various datasets with different data-scale and data-type. For example, we reach top-1 accuracy of 78.45% on CIFAR-100 dataset under the condition of saving $15\times$ parameter memory.

2 Related Works

Recurrent learning algorithms for SNNs. Considering the similarity in computational mechanisms between SNNs and Recurrent Neural Networks (RNNs), Wu *et al.* [44] and Neftci *et al.* [35] transferred the Back-propagation Through Time (BPTT) method from RNNs to the supervised learning field of SNNs and utilized surrogate functions to tackle the non-differentiable problem existed in the spike firing process, which is called the STBP training algorithm. On this basis, Li *et al.* [29], Guo *et al.* [14] and Wang *et al.* [43] respectively attempted to start from the perspective of regulating the distribution about the backward gradient and membrane potential, introducing progressive surrogate functions and penalty terms. Deng *et al.* [6] proposed a target learning function which comprehensively considers the SNN output distribution within each time-step, which is particularly suitable for neuromorphic sequential data. To further improve the learning stability and performance of SNNs, various BatchNorm (BN) modules [54, 8, 15, 23] and attention mechanisms

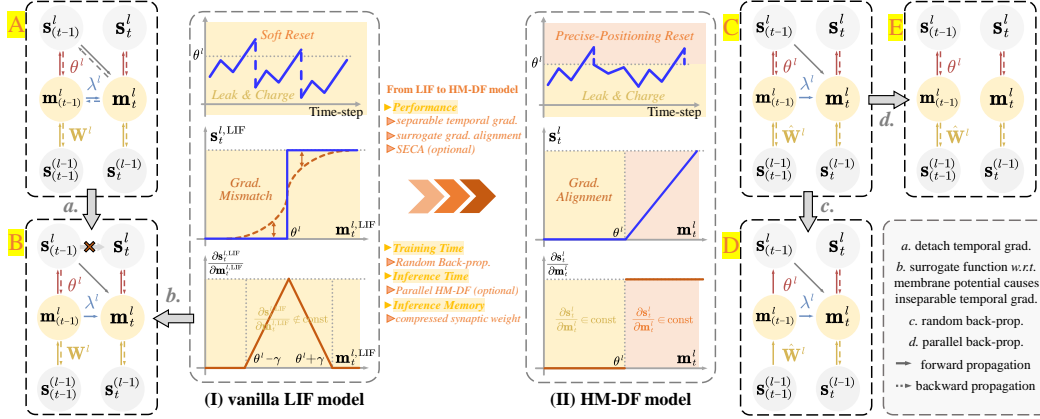


Figure 1: Various training frameworks for SNNs in synaptic and neuron layers. (a): STBP training, (b): vanilla online training based on LIF model, (c)-(e): online training based on HM-DF model.

[49, 37, 55, 48] have been proposed successively, which capture the representation information contained in spike sequences from multiple dimensions, including spatial-wise, temporal-wise and channel-wise. Recently, advanced spiking models have become a focus of academic attention. Researchers have proposed a variety of neuron models with stronger dynamic properties and memory capabilities around membrane-related parameters [9, 50], firing mechanism [13, 38] and dendrite structure [16, 41], promoting deeper exploration towards brain-inspired intelligence. LIAF-Net [45] adopt a similar model structure to this work and combine it with a series of RNN-related modules, but they aim to achieve lightweight information processing rather than efficient online training and deployment. In addition, a spatial-temporal back-propagation algorithm based on spike firing time [1, 24, 53, 57] has also attracted widespread attention. However, this series of methods are currently limited by high computational complexity and unstable training process, which cannot be effectively applied to complex network backbones and large-scale datasets.

Online learning algorithm for SNNs. Although STBP learning algorithm promotes SNNs to join the club of high-performance models, it also brings severe computational burden to SNNs during the training phase, especially the GPU memory that will increase linearly with the number of time-steps. Xiao *et al.* [46] transferred the idea of online learning to the domain of SNN direct training, which splits the back-propagation chain by ignoring the backward gradients with temporal dependencies, making the training GPU memory independent of time-steps. On this basis, Meng *et al.* [33] proposed a selective back-propagation scheme based on online learning, which significantly improves training efficiency. Yang *et al.* [47] combined online learning with ANN-SNN knowledge distillation, further accelerating the training convergence speed of SNNs. Zhu *et al.* [56] proposed a brand-new BatchNorm module suitable for online learning, which enhances the stability of gradient calculation by considering the global mean and standard deviation in the temporal dimension. To enrich the neurodynamic property of online learning, Jiang *et al.* [22] introduced the difference of membrane potential between adjacent time-steps as a feature term into the backward gradient calculation. Inspired by the architecture of reversed network, Zhang *et al.* [51] and Hu *et al.* [18] respectively proposed reversible memory-efficient training algorithms from spatial and temporal perspectives. This type of algorithm can ensure computational consistency between online and STBP learning under the condition of occupying constant GPU memory, but it requires bi-directional computation towards all intermediate variables, which inevitably increases computational overhead. In addition, it is worth noting that most of the online learning methods mentioned above neglect the optimization of computation time and memory usage during the inference phase, thus failing to demonstrate their advantages over STBP training when deploying SNN models.

3 Preliminaries

Leaky Integrate and Fire (LIF) model. The current mainstream spiking model used in SNN community is LIF model [11], which involves three calculation processes, including charging, firing and resetting. As shown in Eq.(1), at each time-step, LIF model will receive the input current I_t^{LIF}

and refer to the previous residual potential $\mathbf{v}_{(t-1)}^{l,\text{LIF}}$, then accumulate the corresponding membrane potential $\mathbf{m}_t^{l,\text{LIF}}$. When $\mathbf{m}_t^{l,\text{LIF}}$ has exceeded the firing threshold θ^l , a spike $\mathbf{s}_t^{l,\text{LIF}}$ will be transmitted to the post-synaptic layer and $\mathbf{m}_t^{l,\text{LIF}}$ will be reset. Here \mathbf{W}^l denotes the synaptic weight and λ^l represents the membrane leakage parameter.

$$\begin{aligned} \mathbf{m}_t^{l,\text{LIF}} &= \lambda^l \odot \mathbf{v}_{(t-1)}^{l,\text{LIF}} + \mathbf{I}_t^{l,\text{LIF}}, \quad \mathbf{v}_t^{l,\text{LIF}} = \mathbf{m}_t^{l,\text{LIF}} - \mathbf{s}_t^{l,\text{LIF}}, \\ \mathbf{I}_t^{l,\text{LIF}} &= \mathbf{W}^l \mathbf{s}_t^{(l-1),\text{LIF}}, \quad \mathbf{s}_t^{l,\text{LIF}} = \begin{cases} 1, & \mathbf{m}_t^{l,\text{LIF}} \geq \theta^l \\ 0, & \text{otherwise} \end{cases}. \end{aligned} \quad (1)$$

STBP Training. To effectively train LIF model, the back-propagation procedure of SNNs usually chooses to expand along both spatial and temporal dimensions, as shown in Fig.1(a). We use \mathcal{L} to denote the target loss function. As shown in Eq.(2), $\frac{\partial \mathcal{L}}{\partial \mathbf{m}_t^{l,\text{LIF}}}$ depends on both $\frac{\partial \mathcal{L}}{\partial \mathbf{s}_t^{l,\text{LIF}}}$ and $\frac{\partial \mathcal{L}}{\partial \mathbf{m}_{(t+1)}^{l,\text{LIF}}}$

simultaneously, while the non-differentiable problem of $\frac{\partial \mathbf{s}_t^{l,\text{LIF}}}{\partial \mathbf{m}_t^{l,\text{LIF}}}$ will be tackled through calculating approximate surrogate functions. Although STBP training enables SNN to achieve relatively superior performance, it inevitably causes severe memory overhead during the training process, which will increase linearly with the number of time-steps.

$$\begin{aligned} \frac{\partial \mathcal{L}}{\partial \mathbf{m}_t^{l,\text{LIF}}} &= \underbrace{\frac{\partial \mathcal{L}}{\partial \mathbf{s}_t^{l,\text{LIF}}} \frac{\partial \mathbf{s}_t^{l,\text{LIF}}}{\partial \mathbf{m}_t^{l,\text{LIF}}}}_{\text{spatial dimension}} + \underbrace{\frac{\partial \mathcal{L}}{\partial \mathbf{m}_{(t+1)}^{l,\text{LIF}}} \frac{\partial \mathbf{m}_{(t+1)}^{l,\text{LIF}}}{\partial \mathbf{m}_t^{l,\text{LIF}}}}_{\text{temporal dimension}}. \\ \nabla_{\mathbf{W}^l} \mathcal{L} &= \sum_{t=1}^T \frac{\partial \mathcal{L}}{\partial \mathbf{m}_t^{l,\text{LIF}}} \frac{\partial \mathbf{m}_t^{l,\text{LIF}}}{\partial \mathbf{W}^l}, \quad \frac{\partial \mathbf{m}_{(t+1)}^{l,\text{LIF}}}{\partial \mathbf{m}_t^{l,\text{LIF}}} = \lambda^l + \frac{\partial \mathbf{m}_{(t+1)}^{l,\text{LIF}}}{\partial \mathbf{s}_t^{l,\text{LIF}}} \frac{\partial \mathbf{s}_t^{l,\text{LIF}}}{\partial \mathbf{m}_t^{l,\text{LIF}}}. \end{aligned} \quad (2)$$

Online Training. To avoid the issue of training memory overhead, a feasible solution is to ignore $\frac{\partial \mathcal{L}}{\partial \mathbf{m}_{(t+1)}^{l,\text{LIF}}} \frac{\partial \mathbf{m}_{(t+1)}^{l,\text{LIF}}}{\partial \mathbf{m}_t^{l,\text{LIF}}}$ during the gradient calculation process, thereby making the back-propagation chain independent in the temporal dimension, as illustrated in Fig.1(b). Online training enables SNNs to update gradients at any time-step, keeping the GPU memory at a constant level.

4 Methods

4.1 Overcoming the back-propagation discrepancy of online training

From Eq.(2), one can find that the backward gradient of STBP training can also be rewritten as $\frac{\partial \mathcal{L}}{\partial \mathbf{m}_t^{l,\text{LIF}}} = \sum_{i=t}^T \frac{\partial \mathcal{L}}{\partial \mathbf{s}_i^{l,\text{LIF}}} \frac{\partial \mathbf{s}_i^{l,\text{LIF}}}{\partial \mathbf{m}_i^{l,\text{LIF}}} \prod_{j=t+1}^i \frac{\partial \mathbf{m}_j^{l,\text{LIF}}}{\partial \mathbf{m}_{(j-1)}^{l,\text{LIF}}}$. On this basis, we point out the concept of *Separable Backward Gradient*:

Definition 4.1. Assume $\frac{\partial \mathcal{L}}{\partial \mathbf{s}_1^{l,\text{LIF}}} = \dots = \frac{\partial \mathcal{L}}{\partial \mathbf{s}_T^{l,\text{LIF}}}$, if $\forall t \in [1, T]$, the surrogate gradient of $\mathbf{s}_t^{l,\text{LIF}}$ w.r.t. $\mathbf{m}_t^{l,\text{LIF}}$ remains constant, we will have $\frac{\partial \mathcal{L}}{\partial \mathbf{m}_t^{l,\text{LIF}}} = \frac{\partial \mathcal{L}}{\partial \mathbf{s}_t^{l,\text{LIF}}} \sum_{i=t}^T \epsilon^l[i, t]$, here $\epsilon^l[i, t]$ denotes the temporal gradient contribution weight of the i -th step w.r.t. the t -th step, which is a constant value:

$$\epsilon^l[i, t] \in \begin{cases} \frac{\partial \mathbf{s}_i^{l,\text{LIF}}}{\partial \mathbf{m}_i^{l,\text{LIF}}} \prod_{j=t+1}^i \frac{\partial \mathbf{m}_j^{l,\text{LIF}}}{\partial \mathbf{m}_{(j-1)}^{l,\text{LIF}}}, & i > t; \\ \frac{\partial \mathbf{s}_t^{l,\text{LIF}}}{\partial \mathbf{m}_t^{l,\text{LIF}}}, & i = t. \end{cases}$$

Then we can further have $\left(\frac{\partial \mathcal{L}}{\partial \mathbf{m}_t^{l,\text{LIF}}} \right)_{\text{Online}} \Leftrightarrow \left(\frac{\partial \mathcal{L}}{\partial \mathbf{m}_t^{l,\text{LIF}}} \right)_{\text{STBP}}$. Here \Leftrightarrow denotes bidirectional equivalence. The gradient at this point is called *Separable Backward Gradient*.

When the precondition of Definition 4.1 holds true, the back-propagation chain can be considered separable in the temporal dimension and the backward gradient of online training can be seamlessly transformed from that of STBP training. Unfortunately, as shown in Fig.1(I), vanilla STBP training generally requires surrogate gradient functions which are related to the membrane potential value (e.g. Triangle Function: $\frac{\partial \mathbf{s}_t^{l,\text{LIF}}}{\partial \mathbf{m}_t^{l,\text{LIF}}} = \frac{1}{\gamma^2} \max(\gamma - |\mathbf{m}_t^{l,\text{LIF}} - \theta^l|, 0)$), to provide richer information for binary spikes with limited representation capabilities. Therefore, current online training cannot fully

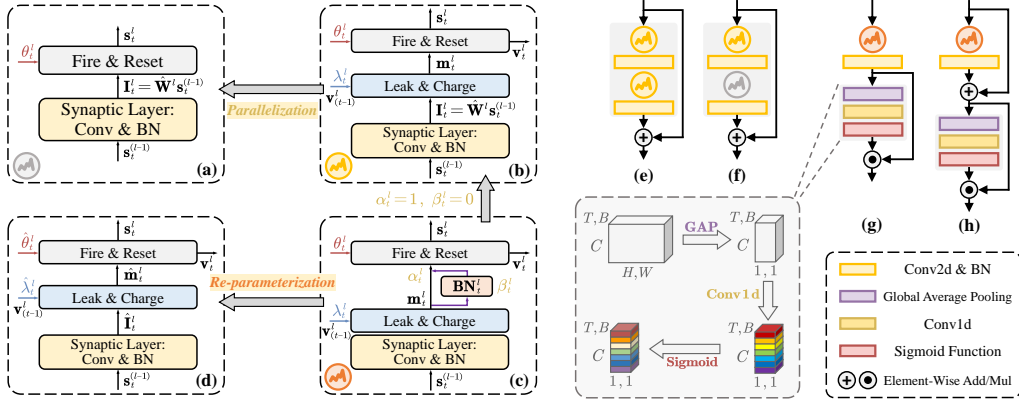


Figure 2: Various versions and blocks of HM-DF model. (a): parallel computation, (b): learnable membrane-parameters, (c): membrane potential batch-normalization, (d) the model after re-parameterization in the inference stage; (e): vanilla residual block, (f): parallel acceleration block, (g)-(h): blocks based on SECA.

overcome the discrepancy between forward and backward propagation, which also limits its learning precision.

To tackle this problem, we propose the HM-DF model, which is a set of advanced spiking models suitable for online training. As shown in Eq.(3) and Fig.1(II), compared to vanilla LIF model, HM-DF model retains the inherent membrane potential calculation mechanism of spiking models within the region below θ^l , while introducing a novel reset mechanism called Precise-Positioning Reset (P2-Reset) in the region above θ^l . Specifically, after each firing process, HM-DF model will reset the amplitude of v^l to θ^l and transmit spikes with values of $m^l - \theta^l$ to the posterior layer:

$$\begin{aligned} \mathbf{m}_t^l &= \lambda_t^l \odot \mathbf{v}_{(t-1)}^l + \mathbf{I}_t^l, \quad \mathbf{v}_t^l = \mathbf{m}_t^l - \mathbf{s}_t^l, \quad \mathbf{I}_t^l = \hat{\mathbf{W}}^l \mathbf{s}_t^{(l-1)}, \\ \mathbf{s}_t^l &= \begin{cases} \mathbf{m}_t^l - \theta_t^l, & \mathbf{m}_t^l \geq \theta_t^l \\ 0, & \text{otherwise} \end{cases} = \text{ReLU}(\mathbf{m}_t^l - \theta_t^l). \end{aligned} \quad (3)$$

Here $\hat{\mathbf{W}}^l$ adopts the learning modes of 1-bit [30] or 1.5-bit [27], which compresses the synaptic weight to a ultra-low number of bits to reduce computational overhead. Specifically, the 1-bit scheme ($\{-1, +1\}$) aims to obtain the spiking model with optimal memory compression, while the 1.5-bit scheme ($\{0, \pm 1\}$) effectively reduces the calculation number of spike events and power consumption by promoting the sparsity in synaptic weights. According to Eq.(3), we can further derive the back-propagation chain of HM-DF model during the online training process:

$$\nabla_{\hat{\mathbf{W}}^l} \mathcal{L} = \sum_{t=1}^T \frac{\partial \mathcal{L}}{\partial \mathbf{m}_t^l} \frac{\partial \mathbf{m}_t^l}{\partial \mathbf{W}^l} \frac{\partial \mathbf{W}^l}{\partial \hat{\mathbf{W}}^l}, \quad \frac{\partial \mathcal{L}}{\partial \mathbf{m}_t^l} = \frac{\partial \mathcal{L}}{\partial \mathbf{s}_t^l} \frac{\partial \mathbf{s}_t^l}{\partial \mathbf{m}_t^l}. \quad (4)$$

Here we make an analysis from the perspective of Defect (i) and (iii). Firstly, we can convert the non-differentiable firing process into $\mathbf{s}_t^l = \text{ReLU}(\mathbf{m}_t^l - \theta_t^l)$ at this point, which will achieve completely precise backward gradient alignment. Furthermore, $\frac{\partial \mathbf{s}_t^l}{\partial \mathbf{m}_t^l}$ remains constant in $(-\infty, \theta_t^l]$ and $(\theta_t^l, +\infty)$ respectively, which makes the surrogate gradients of HM-DF model independent of the corresponding membrane potential value.

Considering the unique properties of HM-DF model in terms of spike firing mechanism and surrogate gradient values, we can further propose the following theorem:

Theorem 4.2. *In the following two cases, the back-propagation of HM-DF model satisfies the condition of Separable Backward Gradient and $\forall i > t, \epsilon^l[i, t] = \mathbf{0}$:*

- (i) $\mathbf{I}_1^l \geq \theta_1^l - \lambda_1^l \mathbf{v}_0^l; \forall t \geq 2, \mathbf{I}_t^l \geq \theta_t^l - \lambda_t^l \mathbf{v}_{(t-1)}^l$.
- (ii) $\forall t \in [1, T], \mathbf{I}_t^l < \theta_t^l - \lambda_t^l \mathbf{v}_{(t-1)}^l$.

From Theorem 4.2, one can find that HM-DF model can reduce the discrepancy between forward and backward propagation more effectively. On this basis, we set learnable membrane leakage parameters

Table 1: Comparison of computational overhead among various learning frameworks during the training and inference phases.

Method	Random BP	Parallel Comput.	Train. Time	Train. Mem.	Inf. Time	Inf. Mem.
STBP Training	N/A	N/A	✗	✗	✗	✗
Online Training	✗	N/A	✗	✓	✗	✗
	✓	N/A	✓	✓	✗	✗
Ours	✗	✗	✗	✓	✗	✓
	✓	✗	✓	✓	✗	✓
	✓	✓	✓	✓	✓	✓

λ_t^l and thresholds θ_t^l for HM-DF model at each time-step, enabling HM-DF model to more adaptively regulate the separability of its learning gradient during online training, as shown in Fig.2(b).

4.2 HM-DF model with membrane potential batch-normalization

In HM-DF model, the distribution of \mathbf{m}_t^l plays a crucial role: on the one hand, it affects the distribution of input current $[\mathbf{I}_t^{(l+1)}, \dots, \mathbf{I}_T^{(l+1)}]$ in the posterior layer at the current and subsequent time-steps; on the other hand, it regulates the distribution of surrogate gradients $[\frac{\partial s_t^l}{\partial \mathbf{m}_t^l}, \dots, \frac{\partial s_T^l}{\partial \mathbf{m}_T^l}]$. From Definition 4.1 and Theorem 4.2, we can note that the above two aspects will jointly determine the separability degree of the backward gradient during the online training process, thereby indirectly affecting the learning performance of SNNs. Therefore, based on the vanilla HM-DF model, we propose a novel version that enables to regulate \mathbf{m}_t^l through membrane potential batch-normalization:

$$\begin{aligned} \mathbf{m}_t^l &= \lambda_t^l \odot \mathbf{v}_{(t-1)}^l + \mathbf{I}_t^l, \quad \hat{\mathbf{m}}_t^l = \alpha_t^l \odot \mathbf{m}_t^l + \beta_t^l \odot \mathbf{BN}_t^l(\mathbf{m}_t^l), \\ \mathbf{BN}_t^l(\mathbf{m}_t^l) &= \gamma \cdot \frac{\mathbf{m}_t^l - \mu_t}{\sqrt{\sigma_t^2 + \epsilon}} + b, \quad \mathbf{v}_t^l = \hat{\mathbf{m}}_t^l - \mathbf{s}_t^l, \quad \mathbf{s}_t^l = \text{ReLU}(\hat{\mathbf{m}}_t^l - \theta_t^l). \end{aligned} \quad (5)$$

Here μ_t and σ_t are the mean and standard deviation of \mathbf{m}_t^l , while γ and ϵ, b are the scaling and shifting factors of the BatchNorm layer. α_t^l and β_t^l are learnable parameters that regulate the normalization degree of \mathbf{m}_t^l . When $\alpha_t^l = 1, \beta_t^l = 0$, our model will degrade to the vanilla learnable HM-DF model mentioned in Section 4.1, which ensures its performance lower-bound. As illustrated in Fig.2(c), here we assign corresponding $\mathbf{BN}_t^l(\cdot)$ for each time-step, achieving more precise control for membrane potential distribution and gradient separability. At this point, we can rewrite Theorem 4.2 as follow:

Corollary 4.3. *In the following two cases, the back-propagation of HM-DF model (membrane potential batch-normalization version) satisfies the condition of Separable Backward Gradient:*

$$\begin{aligned} (i) \quad \mathbf{I}_1^l &\geq \frac{\sqrt{\sigma_1^2 + \epsilon}(\theta_1^l - \beta_1^l b) + \gamma \beta_1^l \mu_1}{\alpha_1^l \sqrt{\sigma_1^2 + \epsilon} + \gamma \beta_1^l} - \lambda_1^l \mathbf{v}_0^l, \quad \forall t \geq 2, \quad \mathbf{I}_t^l \geq \frac{\sqrt{\sigma_t^2 + \epsilon}(\theta_t^l - \beta_t^l b) + \gamma \beta_t^l \mu_t}{\alpha_t^l \sqrt{\sigma_t^2 + \epsilon} + \gamma \beta_t^l} - \lambda_t^l \theta_{(t-1)}^l, \\ (ii) \quad \forall t \in [1, T], \quad \mathbf{I}_t^l &< \frac{\sqrt{\sigma_t^2 + \epsilon}(\theta_t^l - \beta_t^l b) + \gamma \beta_t^l \mu_t}{\alpha_t^l \sqrt{\sigma_t^2 + \epsilon} + \gamma \beta_t^l} - \lambda_t^l \mathbf{v}_{(t-1)}^l. \end{aligned}$$

In addition, it is worth noting that the HM-DF model based on membrane potential batch-normalization can also be converted into vanilla learnable HM-DF model through re-parameterization during the inference phase, thereby avoiding the introduction of additional computational overhead, as shown in Fig.2(c)-(d). Firstly, we can integrate Eq.(5) into the following equation:

$$\hat{\mathbf{m}}_t^l = \left(\alpha_t^l + \frac{\gamma \cdot \beta_t^l}{\sqrt{\sigma_t^2 + \epsilon}} \right) \mathbf{m}_t^l - \beta_t^l \left(\frac{\gamma \cdot \mu_t}{\sqrt{\sigma_t^2 + \epsilon}} - b \right). \quad (6)$$

Subsequently, we can merge the scaling and shifting terms *w.r.t.* \mathbf{m}_t^l in Eq.(6) into membrane-related parameters at different positions, including membrane leakage parameters, firing threshold, input current and reset process:

$$\begin{aligned} \hat{\lambda}_t^l &= \left(\alpha_t^l + \frac{\gamma \cdot \beta_t^l}{\sqrt{\sigma_t^2 + \epsilon}} \right) \lambda_t^l, \quad \hat{\theta}_t^l = \theta_t^l + \beta_t^l \left(\frac{\gamma \cdot \mu_t}{\sqrt{\sigma_t^2 + \epsilon}} - b \right), \\ \hat{\mathbf{I}}_t^l &= \left(\alpha_t^l + \frac{\gamma \cdot \beta_t^l}{\sqrt{\sigma_t^2 + \epsilon}} \right) \mathbf{I}_t^l, \quad \mathbf{v}_t^l = \mathbf{m}_t^l - \mathbf{s}_t^l - \beta_t^l \left(\frac{\gamma \cdot \mu_t}{\sqrt{\sigma_t^2 + \epsilon}} - b \right). \end{aligned} \quad (7)$$

4.3 Strengthening the performance of online learning and deployment

As illustrated in Fig.1(a)-(b) and Tab.1, compared to STBP training, vanilla online training only saves GPU memory during the training phase, without providing any advantages in terms of computation time or memory overhead during the inference phase, which impedes effective online deployment for trained models. In comparison, we point out that online training based on HM-DF model can achieve full-stage computational optimization:

- **Training Time:** As shown in Fig.1(d), we transfer the idea of Random Back-propagation [33] to the online training of HM-DF model, which means that we randomly select only 1 time-step within T time-steps for each mini-batch data to propagate backward gradient. This technique significantly improves the back-propagation efficiency and reduces the gradient computation load from $O(T)$ to $O(1)$.
- **Training Memory:** Consistent with previous online training methods, as shown in Eq.(4), HM-DF model does not consider the computation of $\frac{\partial \mathbf{m}_{(t+1)}^l}{\partial \mathbf{m}_t^l}$, ensuring that the GPU memory is independent of the number of training time-steps and keeps constant.
- **Inference Time:** We introduce a parallel computation version for HM-DF model to accelerate inference time, as shown in Fig.1(e) and Fig.2(a). This simplified HM-DF model does not take into account residual membrane potential information from previous time-steps, allowing for simultaneous forward calculation for all time-steps. In addition, it does not require $\mathbf{v}_{(t-1)}^l$ to be kept as an intermediate variable during the training process (to update learnable λ_t^l), which further saves training GPU memory.
- **Inference Memory:** Due to P2-Reset, HM-DF model is able to transmit spikes with richer information, this allows us to significantly compress the synaptic weight without sacrificing much learning performance, which makes our model merely occupy minimal memory and become more suitable for online deployment.

4.4 Enhancing online training through channel attention mechanism

Channel Attention mechanism [19, 42, 12] is usually inserted after the convolutional layers to further optimize the network performance. We transfer the idea of ECA [42] to the online training based on HM-DF model, then propose Spiking Efficient Channel Attention (SECA) mechanism, as shown in Eq.(8).

$$\text{SECA}(\mathbf{I}_t^l) = \sigma \left(\underbrace{\text{Conv1d}}_{\in \mathbb{R}^{1 \times 1 \times K}} \left(\underbrace{\text{GAP}(\mathbf{I}_t^l)}_{\in \mathbb{R}^{B \times 1 \times C}} \right) \right) \odot \mathbf{I}_t^l. \quad (8)$$

Here the input current $\mathbf{I}_t^l \in \mathbb{R}^{B \times C \times H \times W}$ will be compressed to $\mathbb{R}^{B \times C \times 1 \times 1}$ through the Global Average Pooling (GAP) layer, then Conv1d(\cdot) and Sigmoid Function $\sigma(\cdot)$ will be used to capture and activate the attention scores among different channels, ultimately merging with the shortcut path. Considering that the HM-DF model can convey enough information representation at each time-step, we enable the spike sequence to share the weight of SECA in the temporal dimension. Due to its extremely low parameter quantity (only 1 Conv1d layer with $1 \times 1 \times K$ parameters), SECA can further enhance the learning ability of SNNs under the condition of hardly affecting its online deployment.

In addition, as shown in Eq.(9) and Fig.2(g)-(h), we further propose two variants for SECA:

$$\text{SECA}_I^l(\cdot) : \text{SECA}(\mathbf{I}_t^l), \text{SECA}_{II}^l(\cdot) : \text{SECA}(\mathbf{I}_t^{(l-1)} + \mathbf{I}_t^l). \quad (9)$$

Here $\text{SECA}_I^l(\cdot)$ is the vanilla channel attention mechanism, while considering the shortcomings of compressed synaptic layers in feature extraction, $\text{SECA}_{II}^l(\cdot)$ combines the input currents from both pre-synaptic and post-synaptic layers to further enhance the effectiveness of the attention mechanism. The overall algorithm procedure based on HM-DF model and related optimization techniques has been summarized in Algorithm 1.

5 Experiments

To validate the superiority of our proposed scheme compared to vanilla online learning framework, we investigate the learning performance of HM-DF model on various datasets with different data-scale

Table 2: Comparison with previous SoTA works on STBP and online training. Here Param.(B) calculates the parameter memory occupied by convolutional and linear layers in the corresponding standard network backbone.

Dataset	Method	Arch.	Param.(B)	Online Train.	T	Acc.(%)
CIFAR-10	STBP-tdBN [54]	ResNet-19	50.48M	✗	4	92.92
	Dspike [29]	ResNet-18	44.66M	✗	4	93.66
	TET [6]	ResNet-19	50.48M	✗	4	94.44
	GLIF [50]	ResNet-18	44.66M	✗	4, 6	94.67, 94.88
	SLTT [33]	ResNet-18	44.66M	✓	6	94.44
	Ours	ResNet-18	2.82M	✓	4	95.59
CIFAR-100	Dspike [29]	ResNet-18	44.84M	✗	4	73.35
	TET [6]	ResNet-19	50.57M	✗	4	74.47
	GLIF [50]	ResNet-18	44.84M	✗	4, 6	76.42, 77.28
	SLTT [33]	ResNet-18	44.84M	✓	6	74.38
	Ours	ResNet-18	3.00M	✓	4	78.45
	ImageNet-200	DCT [10]	VGG-13 [†]	38.02M+	✗	125
Online-LTL [47]		VGG-13	38.02M+	✓	16	54.82
Offline-LTL [47]		VGG-13	38.02M+	✗	16	55.37
ASGL [43]		VGG-13	38.02M	✗	4, 8	56.57, 56.81
Ours		VGG-13	2.77M	✓	4	60.68
ImageNet-1k		STBP-tdBN [54]	ResNet-34	87.12M	✗	6
	TET [6]	ResNet-34	87.12M	✗	6	64.79
	OTTT [46]	ResNet-34	87.12M	✓	6	65.15
	SLTT [33]	ResNet-34	87.12M	✓	6	66.19
	Ours	ResNet-34	10.06M	✓	4	69.77
	DVS-CIFAR10	STBP-tdBN [54]	ResNet-19	50.48M	✗	10
Dspike [29]		ResNet-18	44.66M	✗	10	75.40
OTTT [46]		VGG-SNN	37.05M	✓	10	76.30
NDOT [22]		VGG-SNN	37.05M	✓	10	77.50
Ours		ResNet-18	2.81M	✓	10	81.70
Ours		VGG-SNN	2.49M	✓	10	83.00

[†] utilizes fully-connected layers with relatively large parameter quantity.

and data-type, including CIFAR-10(100) [26], ImageNet-200(1k) [5] and DVS-CIFAR10 [28]. We comprehensively consider previous methods based on STBP and online training as our comparative works for ResNet [17, 20] and VGG [40] backbones. Training and implementation details have been provided in Appendix.

5.1 Comparison with previous SoTA works

CIFAR-10 & CIFAR-100. As shown in Tab.2, compared to conventional STBP and online learning framework, our scheme utilizes P2-Reset mechanism and synaptic weight compression technique, which saves approximately 15× synaptic parameter memory without performance degradation, enabling effective online deployment for SNN models. In addition, we achieve higher learning precision within the same or fewer time-steps. For example, our method outperforms GLIF [50] and SLTT [33] with accuracies of 2.03% and 4.07% respectively on CIFAR-100, ResNet-18.

ImageNet-200 & ImageNet-1k. For large-scale datasets, our HM-DF model has also demonstrated significant advantages. For instance, we respectively achieve accuracies of 60.68% and 69.77% on ImageNet-200 and ImageNet-1k, which exceeds the corresponding online learning methods [47, 33] within fewer time-steps and saves more than 88% of synaptic parameter memory.

DVS-CIFAR10. Our method can also achieve effective information extraction for neuromorphic data. From Tab.2, one can note that our learning precision is 6.30% higher than Dspike [29] and 5.50% higher than NDOT [22] under the condition of utilizing the identical network backbone and time-steps.

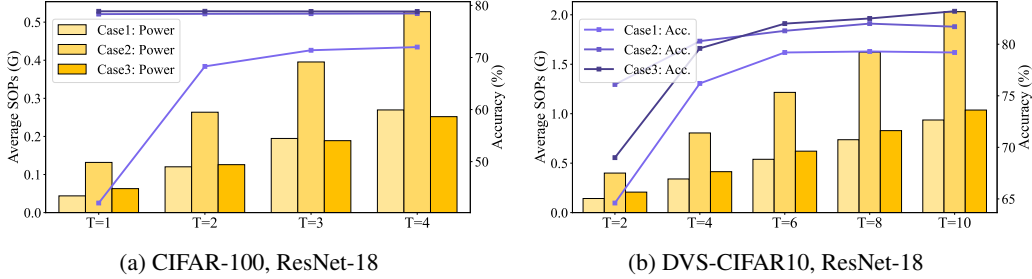


Figure 3: Comparison of accuracy and power consumption for different online learning frameworks in the inference phase. Here Case1 denotes vanilla online learning, Cases 2-3 represent our schemes with 1/1.5-bit synaptic weights, respectively.

Table 3: Parameter memory and accuracy of SNN models before and after utilizing SECA.

Method	CIFAR-10, ResNet-18		CIFAR-100, ResNet-18		DVS-CIFAR10, ResNet-18	
	Param.(B)	Acc.(%)	Param.(B)	Acc.(%)	Param.(B)	Acc.(%)
HM-DF model	2.82M	95.59	3.00M	78.45	2.81M	81.70
HM-DF model (+SECA)	2.82M	95.91 (+0.32)	3.00M	79.33 (+0.88)	2.81M	83.50 (+1.80)

5.2 Validation study for power consumption

In Figure 3, we compare the power consumption of online learning frameworks based on conventional and HM-DF paradigms. Generally speaking, the configuration employing 1-bit synaptic weights exhibits higher energy consumption, while schemes utilizing 1.5-bit precision and standard online training demonstrate comparable levels of power usage. However, for static datasets, it is worth noting that methods from HM-DF family can typically achieve accuracies comparable to the reported SoTA performance within 1 time-step. Furthermore, they outperform standard online training on neuromorphic data when evaluated over the same number of time-steps. Therefore, the HM-DF online learning framework can actually achieve equivalent performance to vanilla online training while incurring lower power consumption. For example, our 1/1.5-bit schemes can achieve superior performance of 78.33/78.87% with only 0.13/0.06G average Synaptic Operations (SOPs), while vanilla online training has already generated 0.27G average SOPs when reaching an accuracy of 72.00%, as shown in Fig.3(a).

5.3 Performance analysis for SECA

As shown in Tab.3, we explore the network performance before and after inserting SECA modules for multiple datasets. One can note that SECA hardly introduces additional parameter quantity, but can provide extra precision improvement for synaptic layers. Among them, after introducing SECA mechanism, the performance improvement of HM-DF online learning on DVS-CIFAR10, ResNet-18 even reaches 1.80%, which effectively compensates for the potential accuracy loss caused by the compression of synaptic weights.

6 Conclusions

In this paper, we systematically analyze the deficiencies of conventional online training, then propose a novel online learning framework based on HM-DF model, which effectively tackles the performance degradation problem caused by gradient dependence and mismatch. Under the condition of maintaining low power consumption, HM-DF model can achieve comprehensive model learning and deployment by flexibly combining various optimization techniques. Experimental results have verified that our proposed scheme can break through the limitations of previous methods and provide further inspiration for the future development of online learning.

References

- [1] Sander M Bohte, Joost N Kok, and Han La Poutre. Error-backpropagation in temporally encoded networks of spiking neurons. *Neurocomputing*, 48(1-4):17–37, 2002.
- [2] Léon Bottou. Stochastic gradient descent tricks. In *Neural networks: Tricks of the trade*, pages 421–436. Springer, 2012.
- [3] Ekin D Cubuk, Barret Zoph, Dandelion Mane, Vijay Vasudevan, and Quoc V Le. Autoaugment: Learning augmentation strategies from data. In *IEEE Conference on Computer Vision and Pattern Recognition*, 2019.
- [4] Mike Davies, Narayan Srinivasa, Tsung-Han Lin, Gautham Chinya, Yongqiang Cao, Sri Harsha Choday, Georgios Dimou, Prasad Joshi, Nabil Imam, Shweta Jain, et al. Loihi: A neuromorphic manycore processor with on-chip learning. *IEEE Micro*, 38(1):82–99, 2018.
- [5] Jia Deng, Richard Socher, Lijia Li, Kai Li, and Feifei Li. Imagenet: A large-scale hierarchical image database. In *IEEE Conference on Computer Vision and Pattern Recognition*, 2009.
- [6] Shikuang Deng, Yuhang Li, Shanghang Zhang, and Shi Gu. Temporal efficient training of spiking neural network via gradient re-weighting. *International Conference on Learning Representations*, 2022.
- [7] Terrance DeVries and Graham W Taylor. Improved regularization of convolutional neural networks with cutout. *arXiv preprint arXiv:1708.04552*, 2017.
- [8] Chaoteng Duan, Jianhao Ding, Shiyang Chen, Zhaofei Yu, and Tiejun Huang. Temporal effective batch normalization in spiking neural networks. In *Advances in Neural Information Processing Systems*, 2022.
- [9] Wei Fang, Zhaofei Yu, Yanqi Chen, Timothee Masquelier, Tiejun Huang, and Yonghong Tian. Incorporating learnable membrane time constant to enhance learning of spiking neural networks. In *Proceedings of the IEEE/CVF International Conference on Computer Vision*, 2021.
- [10] Isha Garg, Sayeed Shafayet Chowdhury, and Kaushik Roy. DCT-SNN: Using dct to distribute spatial information over time for low-latency spiking neural networks. In *Proceedings of the IEEE/CVF International Conference on Computer Vision*, 2021.
- [11] Wulfram Gerstner and Werner M Kistler. *Spiking Neuron Models: Single Neurons, Populations, Plasticity*. Cambridge university press, 2002.
- [12] Nianhui Guo, Joseph Bethge, Christoph Meinel, and Haojin Yang. Join the high accuracy club on imagenet with a binary neural network ticket. *arXiv preprint arXiv:2211.12933*, 2022.
- [13] Yufei Guo, Yuanpei Chen, Xiaode Liu, Weihang Peng, Yuhang Zhang, Xuhui Huang, and Zhe Ma. Ternary spike: Learning ternary spikes for spiking neural networks. In *AAAI Conference on Artificial Intelligence*, 2024.
- [14] Yufei Guo, Xinyi Tong, Yuanpei Chen, Liwen Zhang, Xiaode Liu, Zhe Ma, and Xuhui Huang. RecDis-SNN: Rectifying membrane potential distribution for directly training spiking neural networks. In *IEEE Conference on Computer Vision and Pattern Recognition*, 2022.
- [15] Yufei Guo, Yuhang Zhang, Yuanpei Chen, Weihang Peng, Xiaode Liu, Liwen Zhang, Xuhui Huang, and Zhe Ma. Membrane potential batch normalization for spiking neural networks. In *Proceedings of the IEEE/CVF International Conference on Computer Vision*, 2023.
- [16] Zecheng Hao, Xinyu Shi, Zihan Huang, Tong Bu, Zhaofei Yu, and Tiejun Huang. A progressive training framework for spiking neural networks with learnable multi-hierarchical model. In *International Conference on Learning Representations*, 2024.
- [17] Kaiming He, Xiangyu Zhang, Shaoqing Ren, and Jian Sun. Deep residual learning for image recognition. In *IEEE Conference on Computer Vision and Pattern Recognition*, 2016.
- [18] JiaKui Hu, Man Yao, Xuerui Qiu, Yuhong Chou, Yuxuan Cai, Ning Qiao, Yonghong Tian, XU Bo, and Guoqi Li. High-performance temporal reversible spiking neural networks with $O(L)$ training memory and $O(1)$ inference cost. In *International Conference on Machine Learning*, 2024.
- [19] Jie Hu, Li Shen, and Gang Sun. Squeeze-and-excitation networks. In *IEEE Conference on Computer Vision and Pattern Recognition*, 2018.

- [20] Yifan Hu, Lei Deng, Yujie Wu, Man Yao, and Guoqi Li. Advancing spiking neural networks towards deep residual learning. *IEEE Transactions on Neural Networks and Learning Systems*, 36(2):2353–2367, 2024.
- [21] Yulong Huang, Xiaopeng Lin, Hongwei Ren, Haotian Fu, Yue Zhou, Zunchang Liu, Biao Pan, and Bojun Cheng. Clif: Complementary leaky integrate-and-fire neuron for spiking neural networks. In *International Conference on Machine Learning*, 2024.
- [22] Haiyan Jiang, Giulia De Masi, Huan Xiong, and Bin Gu. NDOT: Neuronal dynamics-based online training for spiking neural networks. In *International Conference on Machine Learning*, 2024.
- [23] Haiyan Jiang, Vincent Zoonekynd, Giulia De Masi, Bin Gu, and Huan Xiong. Tab: Temporal accumulated batch normalization in spiking neural networks. In *International Conference on Learning Representations*, 2024.
- [24] Jinseok Kim, Kyungsu Kim, and Jae-Joon Kim. Unifying activation- and timing-based learning rules for spiking neural networks. In *Advances in Neural Information Processing Systems*, 2020.
- [25] Seijoon Kim, Seongsik Park, Byunggook Na, and Sungroh Yoon. Spiking-YOLO: spiking neural network for energy-efficient object detection. In *AAAI Conference on Artificial Intelligence*, 2020.
- [26] Alex Krizhevsky, Geoffrey Hinton, et al. Learning multiple layers of features from tiny images. 2009.
- [27] Fengfu Li, Bin Liu, Xiaoxing Wang, Bo Zhang, and Junchi Yan. Ternary weight networks. *arXiv preprint arXiv:1605.04711*, 2016.
- [28] Hongmin Li, Hanchao Liu, Xiangyang Ji, Guoqi Li, and Luping Shi. Cifar10-dvs: an event-stream dataset for object classification. *Frontiers in Neuroscience*, 11, 2017.
- [29] Yuhang Li, Yufei Guo, Shanghang Zhang, Shikuang Deng, Yongqing Hai, and Shi Gu. Differentiable spike: Rethinking gradient-descent for training spiking neural networks. In *Advances in Neural Information Processing Systems*, 2021.
- [30] Zechun Liu, Zhiqiang Shen, Shichao Li, Koen Helwegen, Dong Huang, and Kwang-Ting Cheng. How do adam and training strategies help bnn optimization. In *International Conference on Machine Learning*, 2021.
- [31] Ilya Loshchilov and Frank Hutter. SGDR: stochastic gradient descent with warm restarts. In *International Conference on Learning Representations*, 2017.
- [32] Wolfgang Maass. Networks of spiking neurons: the third generation of neural network models. *Neural Networks*, 10(9):1659–1671, 1997.
- [33] Qingyan Meng, Mingqing Xiao, Shen Yan, Yisen Wang, Zhouchen Lin, and Zhiquan Luo. Towards memory and time-efficient backpropagation for training spiking neural networks. In *Proceedings of the IEEE/CVF International Conference on Computer Vision*, 2023.
- [34] Paul A Merolla, John V Arthur, Rodrigo Alvarez-Icaza, Andrew S Cassidy, Jun Sawada, Filipp Akopyan, Bryan L Jackson, Nabil Imam, Chen Guo, Yutaka Nakamura, et al. A million spiking-neuron integrated circuit with a scalable communication network and interface. *Science*, 345(6197):668–673, 2014.
- [35] Emre O Neftci, Hesham Mostafa, and Friedemann Zenke. Surrogate gradient learning in spiking neural networks: Bringing the power of gradient-based optimization to spiking neural networks. *IEEE Signal Processing Magazine*, 36(6):51–63, 2019.
- [36] Jing Pei, Lei Deng, Sen Song, Mingguo Zhao, Youhui Zhang, Shuang Wu, Guanrui Wang, Zhe Zou, Zhenzhi Wu, Wei He, et al. Towards artificial general intelligence with hybrid tianjic chip architecture. *Nature*, 572(7767):106–111, 2019.
- [37] Xuerui Qiu, Rui-Jie Zhu, Yuhong Chou, Zhaorui Wang, Liang-jian Deng, and Guoqi Li. Gated attention coding for training high-performance and efficient spiking neural networks. In *AAAI Conference on Artificial Intelligence*, 2024.
- [38] Guobin Shen, Dongcheng Zhao, Tenglong Li, Jindong Li, and Yi Zeng. Are conventional snns really efficient? a perspective from network quantization. In *IEEE Conference on Computer Vision and Pattern Recognition*, 2024.

- [39] Xinyu Shi, Zecheng Hao, and Zhaofei Yu. Spikingresformer: Bridging resnet and vision transformer in spiking neural networks. In *IEEE Conference on Computer Vision and Pattern Recognition*, 2024.
- [40] Karen Simonyan and Andrew Zisserman. Very deep convolutional networks for large-scale image recognition. *arXiv preprint arXiv:1409.1556*, 2014.
- [41] Lihao Wang and Zhaofei Yu. Autaptic synaptic circuit enhances spatio-temporal predictive learning of spiking neural networks. In *International Conference on Machine Learning*, 2024.
- [42] Qilong Wang, Banggu Wu, Pengfei Zhu, Peihua Li, Wangmeng Zuo, and Qinghua Hu. Eca-net: Efficient channel attention for deep convolutional neural networks. In *IEEE Conference on Computer Vision and Pattern Recognition*, 2020.
- [43] Ziming Wang, Runhao Jiang, Shuang Lian, Rui Yan, and Huajin Tang. Adaptive smoothing gradient learning for spiking neural networks. In *International Conference on Machine Learning*, 2023.
- [44] Yujie Wu, Lei Deng, Guoqi Li, Jun Zhu, and Luping Shi. Spatio-temporal backpropagation for training high-performance spiking neural networks. *Frontiers in Neuroscience*, 12:331, 2018.
- [45] Zhenzhi Wu, Hehui Zhang, Yihan Lin, Guoqi Li, Meng Wang, and Ye Tang. LIAF-Net: Leaky integrate and analog fire network for lightweight and efficient spatiotemporal information processing. *IEEE Transactions on Neural Networks and Learning Systems*, 33(11):6249–6262, 2021.
- [46] Mingqing Xiao, Qingyan Meng, Zongpeng Zhang, Di He, and Zhouchen Lin. Online training through time for spiking neural networks. In *Advances in Neural Information Processing Systems*, 2022.
- [47] Qu Yang, Jibin Wu, Malu Zhang, Yansong Chua, Xinchao Wang, and Haizhou Li. Training spiking neural networks with local tandem learning. In *Advances in Neural Information Processing Systems*, 2022.
- [48] Man Yao, Jiakui Hu, Tianxiang Hu, Yifan Xu, Zhaokun Zhou, Yonghong Tian, Bo Xu, and Guoqi Li. Spike-driven transformer v2: Meta spiking neural network architecture inspiring the design of next-generation neuromorphic chips. In *International Conference on Learning Representations*, 2024.
- [49] Man Yao, Guangshe Zhao, Hengyu Zhang, Yifan Hu, Lei Deng, Yonghong Tian, Bo Xu, and Guoqi Li. Attention spiking neural networks. *IEEE Transactions on Pattern Analysis and Machine Intelligence*, 45(8):9393–9410, 2023.
- [50] Xingting Yao, Fanrong Li, Zitao Mo, and Jian Cheng. GLIF: A unified gated leaky integrate-and-fire neuron for spiking neural networks. In *Advances in Neural Information Processing Systems*, 2022.
- [51] Hong Zhang and Yu Zhang. Memory-efficient reversible spiking neural networks. In *AAAI Conference on Artificial Intelligence*, 2024.
- [52] Hongyi Zhang, Moustapha Cisse, Yann N Dauphin, and David Lopez-Paz. mixup: Beyond empirical risk minimization. *arXiv preprint arXiv:1710.09412*, 2017.
- [53] Wenrui Zhang and Peng Li. Temporal spike sequence learning via backpropagation for deep spiking neural networks. In *Advances in Neural Information Processing Systems*, 2020.
- [54] Hanle Zheng, Yujie Wu, Lei Deng, Yifan Hu, and Guoqi Li. Going deeper with directly-trained larger spiking neural networks. In *AAAI Conference on Artificial Intelligence*, 2021.
- [55] Zhaokun Zhou, Yuesheng Zhu, Chao He, Yaowei Wang, Shuicheng Yan, Yonghong Tian, and Yuan Li. Spikformer: When spiking neural network meets transformer. In *International Conference on Learning Representations*, 2023.
- [56] Yaoyu Zhu, Jianhao Ding, Tiejun Huang, Xiaodong Xie, and Zhaofei Yu. Online stabilization of spiking neural networks. In *International Conference on Learning Representations*, 2024.
- [57] Yaoyu Zhu, Wei Fang, Xiaodong Xie, Tiejun Huang, and Zhaofei Yu. Exploring loss functions for time-based training strategy in spiking neural networks. In *Advances in Neural Information Processing Systems*, 2023.

A Appendix

A.1 Experimental configuration

For experimental cases in Tabs.2-3, we choose Stochastic Gradient Descent [2] as our optimizer and Cosine Annealing [31] as our scheduler. The initial learning rate and weight decay are respectively set to 0.025 and 0 for ImageNet-1k, 0.01 and 5×10^{-4} for other cases. We consider various data augmentation techniques, including Auto-Augment [3], Cutout [7], and Mixup [52]. The calculation of average SOPs in Fig.3 refers to [55] and is oriented towards convolutional layers. For ResNet backbone, we generally choose the acceleration block as mentioned in Fig.2(f). For VGG structure, we utilize the version of Fig.2(b) for ImageNet-200 and the version of Fig.2(c) for DVS-CIFAR10. For experimental cases based on SECA, we typically choose the combination of Fig.2(a) and Fig.2(g)-(h). More detailed experimental configuration has been provided in Tab.S1.

Table S1: Detailed experimental setup for all training cases.

Method	Arch.	Weight Bit	SECA	Batchsize	Epochs	Fig.2(b)	Fig.2(c)	Fig.2(a)
CIFAR-10	ResNet-18	1	✗	64	300	✓	-	✓
		1	✓			-	✓	
CIFAR-100	ResNet-18	1/1.5	✗	64	300	✓	-	✓
		1	✓			-	✓	
ImageNet-200	VGG-13	1	✗	64	300	✓	-	-
ImageNet-1k	ResNet-34	1.5	✗	256	300	✓	-	✓
DVS-CIFAR10	ResNet-18	1/1.5	✗	32	300	-	✓	✓
		1	✓			-	✓	
	VGG-SNN	1	✗			-	✓	-

A.2 Proof of Theorem 4.2

Theorem 4.2 *In the following two cases, the back-propagation of HM-DF model satisfies the condition of Separable Backward Gradient and $\forall i > t, \epsilon^l[i, t] = \mathbf{0}$:*

- (i) $\mathbf{I}_1^l \geq \theta_1^l - \lambda_1^l \mathbf{v}_0^l; \forall t \geq 2, \mathbf{I}_t^l \geq \theta_t^l - \lambda_t^l \theta_{(t-1)}^l$.
- (ii) $\forall t \in [1, T], \mathbf{I}_t^l < \theta_t^l - \lambda_t^l \mathbf{v}_{(t-1)}^l$.

Proof. For case (i), HM-DF model will emit a spike at each time-step, which means that $\forall t \in [1, T], \frac{\partial s_t^l}{\partial \mathbf{m}_t^l} = 1$. Combining with the definition of $\epsilon^l[i, t]$, we will have:

$$\begin{aligned}
 \epsilon^l[i, t] &= \frac{\partial s_i^l}{\partial \mathbf{m}_i^l} \prod_{j=t+1}^i \frac{\partial \mathbf{m}_j^l}{\partial \mathbf{m}_{(j-1)}^l} \\
 &= \mathbf{1} \cdot \prod_{j=t+1}^i \left(\lambda_j^l + \frac{\partial \mathbf{m}_j^l}{\partial s_{(j-1)}^l} \frac{\partial s_{(j-1)}^l}{\partial \mathbf{m}_{(j-1)}^l} \right) \\
 &= \mathbf{1} \cdot \prod_{j=t+1}^i (\lambda_j^l - \lambda_j^l \cdot \mathbf{1}) \\
 &= \mathbf{0}.
 \end{aligned} \tag{S1}$$

For case (ii), HM-DF model will keep silent at each time-step, which means that $\forall t \in [1, T], \frac{\partial s_t^l}{\partial \mathbf{m}_t^l} = 0$. Combining with Eq.(S1), we will obviously conclude that $\forall i > t, \epsilon^l[i, t] = \mathbf{0}$:

$$\epsilon^l[i, t] = \mathbf{0} \cdot \prod_{j=t+1}^i \left(\lambda_j^l + \frac{\partial \mathbf{m}_j^l}{\partial s_{(j-1)}^l} \frac{\partial s_{(j-1)}^l}{\partial \mathbf{m}_{(j-1)}^l} \right) = \mathbf{0}. \tag{S2}$$

□

A.3 Pseudo Code for HM-DF Online Learning Framework

Algorithm 1 Online training & deployment process for HM-DF model.

Require: SNN model $f_{\text{SNN}}(\mathbf{W}, \lambda, \theta, \alpha, \beta)$ with L layers; Dataset D ; Training time-steps T .

Ensure: Deployable SNN model $f_{\text{SNN}}(\hat{\mathbf{W}}, \hat{\lambda}, \hat{\theta})$.

Online Training Stage

for (Image, Label) in D do

for $t = 1$ to T do

for $l = 1$ to L do

if Use the version of Fig.2(b) **then**

 perform forward propagation in Eq.(3)

else if Use the version of Fig.2(c) **then**

 perform forward propagation in Eq.(5)

else if Use the version of Fig.2(a) **then**

$s_t^l = \text{ReLU}(\hat{\mathbf{W}}^l s_t^{(l-1)} - \theta_t^l)$

end if

if Use SECA modules in Fig.2(g)-(h) **then**

 calculate and merge the channel attention scores through Eqs.(8)-(9)

end if

end for

if Use vanilla BP or the time of Random BP is equal to t **then**

 perform back-propagation as shown in Eq.(4) and update all learnable membrane-related parameters $\lambda_t, \theta_t, \alpha_t, \beta_t, \mathbf{BN}_t(\cdot)$

end if

end for

end for

Online Deployment Stage

for $t = 1$ to $T, l = 1$ to L do

if Use the version of Fig.2(c) **then**

 re-parameterize $\lambda_t^l, \theta_t^l, \alpha_t^l, \beta_t^l, \mathbf{BN}_t^l(\cdot)$ into $\hat{\lambda}_t^l, \hat{\theta}_t^l, \hat{\mathbf{I}}_t^l$ through Eq.(7)

end if

end for

Return $f_{\text{SNN}}(\hat{\mathbf{W}}, \hat{\lambda}, \hat{\theta})$.
